ISSN 1330-3651 (Print), ISSN 1848-6339 (Online) https://doi.org/10.17559/TV-20240319001414
Original scientific paper

Research on the Method of Using Wireless Sensing to Detect Indoor People during Fire Based on Unmanned Aerial Vehicle

Lin TANG, Chao WANG*, Yinfan DING, Meng ZHOU

Abstract: Though improving the efficiency of urban land use, high-rise buildings greatly increase the difficulty in search and rescue during fires. Therefore, effective search and rescue in high-rise building fires has always been a hot and difficult issue in emergency management. Starting from the characteristics of high-rise building fires and the difficulties in addressing them, this paper introduced unmanned aerial vehicle (UAV) technology into search and rescue operations in fires. Based on the influences of dynamic factors on wireless signal (WS) states in a static environment, it investigated the techniques for extracting and sensing wireless channel state features when indoor personnel waves for help and proposed a method for indoor personnel detection based on channel state information (CSI) sensing. In the article, a single source wireless device (common Wi-Fi router) is used as the detection terminal to collect the wireless channel state, and the signal sampling, support vector machine (SVM), and other technologies are combined to realize the wireless channel state sensing and classification. The outcomes of the experiment revealed that the suggested approach can effectively succeed in through-wall detection and sensing for indoor personnel calling for help in the event of a fire, with an accuracy of 94.6%. Incorporating the non-invasive, robust, universal, and low-cost characteristics, the method promises broad application values in improving the search and rescue efficiency of firefighters.

Keywords: wireless signal, channel state information, state sensing, through-wall detection

1 INTRODUCTION

With the increasingly faster pace of urbanization in China, the contradiction between people and land has prompted cities to develop in an upward direction, resulting in the emergence of many high-rise buildings. These buildings can reduce the land occupied by housing and save a lot of space for urban development. However, they typically have a complex structure and increasingly narrow distances in between, which poses many hidden dangers to firefighting and rescue [1].

High-rise buildings in major cities generally have a high height, multiple floors, and complex internal structures, which makes it difficult to evacuate personnel timely in the event of a fire. In addition, rescuers have to climb a long distance to ascertain the presence of those unevacuated people, seriously hurting the timeliness of the rescue. Most high-rise buildings are enclosed and windowless, so the thick smoke and heat generated in fires cannot be discharged promptly, leading to their accumulation in atriums, elevators, and cables. The smoke and heat tend to concentrate upwards, forming a chimney effect and quickly spread throughout the entire building. Even if firefighters take an aerial ladder to detect indoor personnel from outside the building, the thick smoke will seriously cloud the visibility.

Therefore, if effective techniques can be used in these smoky environments for indoor personnel detection in high-rise building fires, there is no need for rescuers to enter the rooms with poor visibility. This solution will greatly improve the timeliness and effectiveness of firefighting and rescue and buy more time to save lives.

The key to effective detection lies in the ability to identify through the wall whether people are calling for help in the room. In other words, the problem boils down to effectively identifying human activities beyond visual distance.

As wireless sensing develops, research groups in China and beyond have suggested multiple systems by using this technology to detect and recognize human activities [2]. One of the groups is Dina Katabi's team from MIT who in 2018 proposed a new human pose estimation system, RF-Pose [3]. This system accurately tracked two-dimensional human postures through walls and obstacles using radio signals, converting visual information about people and the environment into radio frequency signals. In 2019, the same team proposed a skeleton-based action recognition system, Aryokee [4], which could detect human behavior despite wall occlusion and poor lighting conditions, solving problems in scenes inaccessible by current vision-based action recognition methods.

In 2020, Dina Katabi's team suggested a novel system called BodyCompass that monitors sleep postures [5], which determines the user's nighttime sleep postures according to radio frequency reflections in the environment. Without requiring the user to wear or touch any sensors, BodyCompass could reduce events like sleep apnea without infringing on user privacy. In the same year, a new type of human re-identification system, RF-ReID [6], was suggested, which utilized radio frequency signals to derive more durable human attributes, such as body size and shape. RF-ReID could function in occlusion and inadequate lighting conditions, thus better-protecting solitude and enabling its increase to privacy-pertinent fields such as healthcare.

Research teams in China have also conducted a large amount of research on wireless perception. For instance, the low-cost, non-invasive, Wi-Fi device-based sleep monitoring system, WiFi-Sleep [7], leveraged the CSI ratio as well as amplitude and phase signals to monitor the four sleep stages. The Wi-Fi-based gait recognition system WiDIGR [8] solved the problem of strong dependence on walking direction in conventional device-free human gait recognition systems. The primary lightweight, around-the-clock, real-time, non-contact human detection system, WiSH [9], extracted simple and efficient attributions from the received signals' time and frequency correlations, which could achieve long-term real-time monitoring of the human body. There have also been some examples of using Wi-Fi for fingerprint localization [10] and adopting frequency modulated continuous-wave (FMCW) radar for high-precision heart rate monitoring

[11].

In early studies on wireless sensing, received signal strength (RSS) [12] was mostly used for crunching and investigation to pinpoint human behavior. In complicated situations, however, the RSS's performance would sharply decline since multipath fading and time dynamics occur. CSI [13], on the other hand, can identify the characteristics of multipath and help investigate and grasp human motions.

This paper proposes an indoor personnel detection method based on CSI wireless perception. Referencing the WSs' propagation theory [14], the method acts as a proof-of-concept model that uses Wi-Fi signals to pinpoint human behavior. Digital signal processing and machine learning are combined to investigate and crunch the CSI data of WSs, thereby achieving through-wall detection.

The main innovations achieved in this paper are as follows:

1) Combined with digital signal processing and machine learning algorithms, the fast training of small samples is realized, and good expected results are achieved.

The challenges of employing wireless signals to detect blind spot are follows:

1) How to filter and remove interference noise from wireless signals;

2) How to use the features of wireless signals to accurately construct a model for detecting human behavior.

2 THE DESIGN OF THE SYSTEM ARCHITECTURE AND ITS IMPLEMENTATION

2.1 The Design of the System Architecture

The detection of indoor personnel necessitates a system that recognizes human behavior based on using wireless input to detect whether any action occurs in the environment within the coverage of Wi-Fi signals. For example, in practical application scenarios such as a building in which a fire occurs, the internal environment should be in a static state. When sustained actions, e.g., a person indoors calling for help, suddenly occur, the system can detect these anomalies and make judgments warning about the presence of indoor personnel behavior. This system uses WSs as the medium for environmental perception, effectively solving the problems of blind spots, susceptibility to environmental factors like lighting, and high equipment costs in video surveillance systems. Taking advantage of the wall penetration feature for WSs, the system can operate normally even within a non-line-of-sight range, thus achieving accurate through-wall detection in special spaces with visual obstacles, such as rooms with dense smoke during a fire.

As shown in Fig. 1, the detection framework of indoor personnel using wireless input functions in the subsequent three phases.

(1) Preprocessing of data: Low-pass filter denoising and principal component analysis (PCA) are applied to the collected raw dataset to guarantee the acquisition of the CSI dataset related to human behavior in the test environment.

(2) The extraction of features: As the CSI dataset relevant to human behavior characteristics varies in distinct environment states, 5 time-domain attributions that can pinpoint each action, namely the median absolute deviation (*MAD*), quartile deviation, maximum, average, and variance, are derived to classify.

(3) Classification: Based on the obtained data features with labeled output, the support vector machine (SVM) is used by the system [15] to learn and generate a training model. During the testing phase, the generated training model is used to determine the current environment state based on unknown data.

2.2 System Implementation Scheme

2.2.1 Data preprocessing

A laptop is used to collect Wi-Fi link packets and obtain the relevant CSI data from the received packets. The method adopts the orthogonal frequency division multiplexing (OFDM) setup and the 1 × 3 multiple input multiple output (MIMO) format. Since the system uses 1 transmitting and 3 receiving antennas, respectively the CSI information is split into 3 data streams, each with 30 subcarriers. In other words, 1 × 3 × 30 = 90 sets of data can be extracted from each packet, which can be represented in Eq. (1).

$$\begin{aligned} CSI^1 &= \left\{CSI^{1,1}, CSI^{1,2}, \ldots, CSI^{1,30}\right\} \\ CSI^2 &= \left\{CSI^{2,1}, CSI^{2,2}, \ldots, CSI^{2,30}\right\} \\ CSI^3 &= \left\{CSI^{3,1}, CSI^{3,2}, \ldots, CSI^{3,30}\right\} \end{aligned} \tag{1}$$

where $CSI^{i,j}$ denotes an arbitrary subcarrier element in each data packet, i denotes the sequence number of the data stream, and j denotes the sequence number of the subcarrier. Experiments have shown that human activities independently impact the three data streams. This system extracts one of the data streams for analysis and uses CSI amplitude values as the system input.

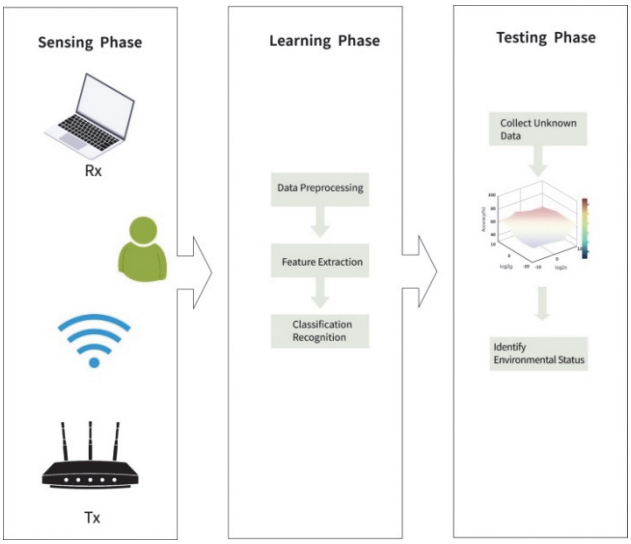

Figure 1 System framework

The transmitter's internal state transitions and the receiver's wireless network cards, e.g., changes in transmission power or internal CSI reference level and transmission rate adaptation, may cause high amplitudes and pulsed noise, which also affects the samples in all data streams. Therefore, the CSI values generated by standard

and commercially available Wi-Fi network cards themselves are noisy, as shown in Fig. 2. To use CSI values to identify human behavior, noise must be disregarded from the CSI time series. The system initially removes the high-frequency noise from the CSI time series through a Butterworth low-pass filter [16]. Because the frequency changes generated by human behavior occur at the spectrum's low frequencies while the noise contains a high frequency, a Butterworth low-pass filter is picked to eliminate the noise. The Butterworth low-pass filter does not cause significant distortions in the signal's phase information but contains the smoothest amplitude response in the passband, so it will not distort the passing signals generated by human behavior. This process removes some high-frequency noise and obtains smoother signal waveforms, as shown in Fig. 3, but there is still some unfiltered noise due to the slow attenuation gain of the Butterworth low-pass filter on the stopband.

The CSI amplitude curves over time of the 5-th, 10-th, 15-th, 20-th, and 25-th subcarriers are selected. Therefore, to derive the most useful information from the CSI time series embedded with residual noise, the system uses the PCA algorithm to extract the filtered subcarrier signal that only contains the channel change information caused by human behavior. The system utilizes this correlation to calculate the principal components of the CSI-TS and then selects them that best represent the general changes in the CSI-TS.

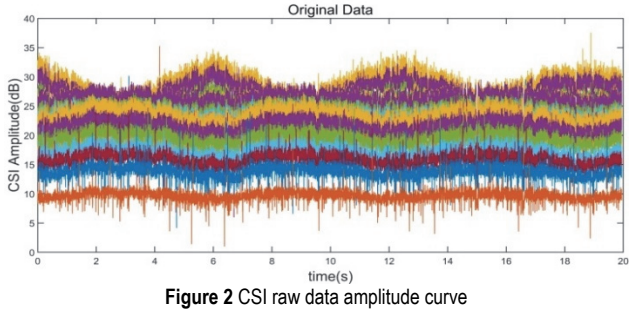

Figure 2 CSI raw data amplitude curve

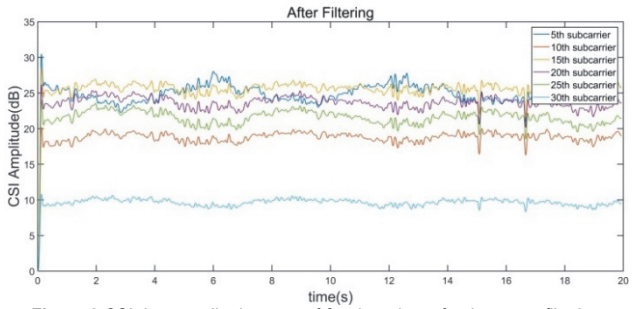

Figure 3 CSI data amplitude curve of 6 subcarriers after low-pass filtering

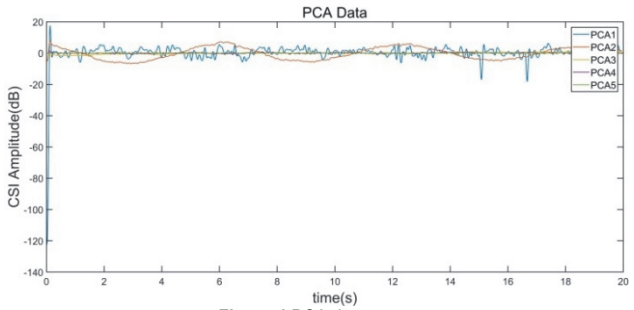

Figure 4 PCA data curve

In PCA, the principal components are arranged in descending order according to variance, so the noise components are ranked first due to their higher variance. Fig. 4 shows the PCA results in static and dynamic environments, respectively, and the first principal component changes significantly and is not related to human motion. Although low-pass filtering could disregard most burst noise in CSI, some noise led by changes in the internal state of Wi-Fi equipment remains. Therefore, the noisiest first principal component is discarded, and the remaining components are used for feature extraction. In a typical PCA matrix, most information is contained in the first p principal components. This system chooses $p = 2$.

2.2.2 Feature Extraction

To distinguish between static and dynamic environments for personnel detection, we need to extract features that can uniquely represent the CSI in each environment. Finally, the following five time-domain features are selected:

(1) *MAD*.

In statistics, a robustness metric, *MAD*, is used for the univariate dataset's bias, which could also denote the generic parameter predicted from the sample's *MAD*. Let $X_1, X_2, \ldots, X_n$ be a univariate data set. *MAD* is delineated as the median of absolute deviations from the data point to the median:

$$MAD = \text{median}\left(\left|X_i - \text{median}(X)\right|\right) \tag{2}$$

where the deviations between the data and the median are initially computed, and the median of the absolute values of these deviations is the *MAD*.

(2) Quartile deviation.

Quartile deviation is the difference between the upper quartile ($Q3$, the number at 75%) and the lower quartile ($Q1$, the number at 25%). This index is mainly used to measure the degree of dispersion for sequential data, and its calculation formula is as follows:

$$Q = Q3 - Q1 \tag{3}$$

Quartile deviation represents the dispersion degree of the middle 50% of the dataset, and the smaller the score, the more concentrated the middle data. In addition, since the median is in the middle part of a dataset, the size of the quartile deviation can to some extent reflect the representativeness of the median for the entire data.

(3) Maximum.

The maximum value in a set of data can normally be determined through sorting.

(4) Mean.

The mean reflects the trend of data concentration. This system uses the arithmetic mean, as calculated by.

$$\bar{x} = \frac{x_1 + x_2 + \ldots + x_n}{n} = \frac{\sum_{i=1}^{n} x_i}{n} \tag{4}$$

(5) Variance.

Variance measures a random variable's dispersion or a dataset, which is employed to characterize the deviation degree between the random variable and its expected value (i.e., average).

The system generates a $1 \times N$ matrix through data preprocessing, where the collected data packet numbers are denoted by N, i.e., the CSI data numbers. A method called sliding window is employed to compute the various time-domain attributions of this matrix. The system sets the sliding window length to 100 and the step size to 60. For each data segment in the sliding window, feature calculations are performed to generate a 5×4000 feature matrix F, where the feature vectors with a sequence number of 1 - 2000 belong to the static environment and the 2001 - 4000 attribution vectors belong to the dynamic environment. The feature matrix F constitutes the classifier's inputs, and the 5 time-domain attributes are shown in Fig. 5 to Fig. 9, respectively. Significantly different patterns can be observed across the red dashed line, indicative of differences in feature data between the static environment and the dynamic environment. Therefore, the system can use the matrix F to pinpoint the test environment's current state.

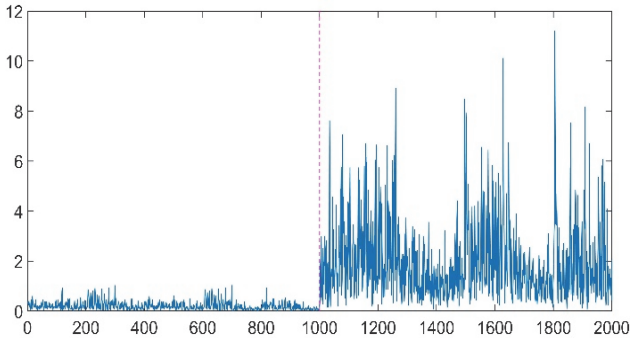

Figure 5 *MAD*

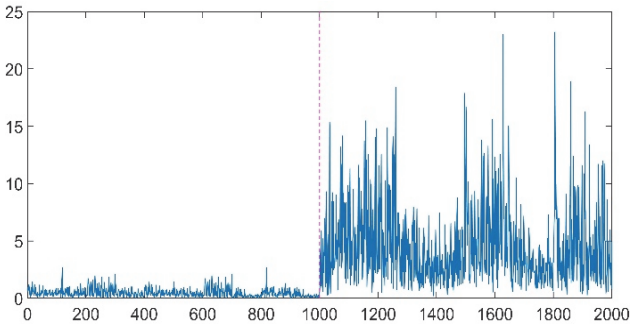

Figure 6 Quartile deviatio

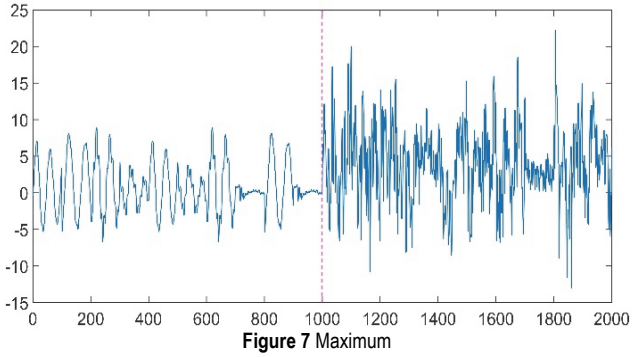

Figure 7 Maximum

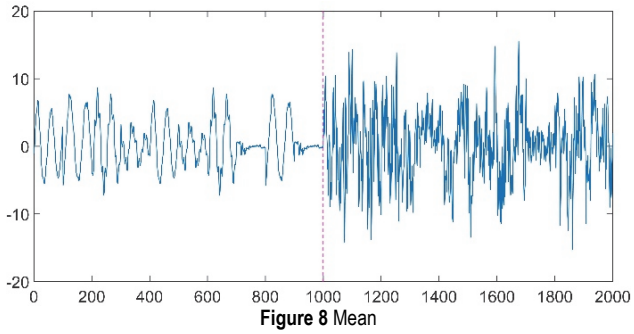

Figure 8 Mean

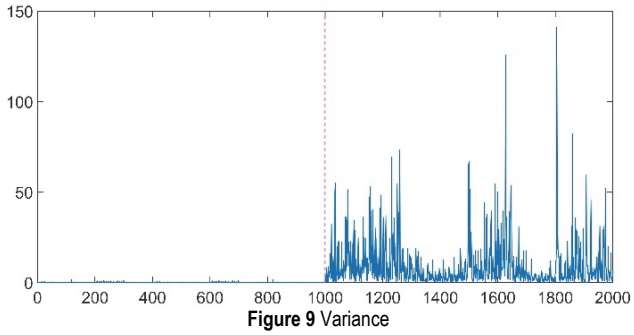

Figure 9 Variance

2.3 Classification

LIBSVM [17] provides a function of cross-validation (CV) in which the radial basis function (RBF) kernel is selected. Eq. (5) presents the decision function.

$$predict_{label} = \mathrm{sgn}\left(\sum_{i=1}^{n} w_i e^{-gamma\|x_i - x\|^2} + b\right) \tag{5}$$

where $e^{-gamma\|x_i - x\|^2}$ denotes the kernel function utilized by the SVM method, x_i, x and, w_i denote the support vectors in the training set, a sample of the labeled data to be estimated, and the support vector's coefficient in the decision function, respectively b denotes the opposite of the constant term in the same function and $predict_{label}$ represents the decision outcome. So, the decision function's parameters are found, the label of the sample can be attained by the system, and the environment's current state is identified.

The kernel function of the RBF has 2 parameters: *Cost*, the parameter of the loss function, abbreviated as C and the RBF parameter *gamma*, abbreviated as g. The C balances incorrectly classified samples and the simplicity of the interface. A large C raises the degree of freedom of the model to choose more support vectors and thus ensures that all samples are correctly classified, while a lower C can better smooth the interface. The g denotes the reciprocal of the influence radius of the support vector sample, representing the influence size by a single training set. The smaller the score g, the larger the impact.

CV is used to evaluate the model prediction result, especially the pre-trained model's performance on a new dataset. The basic idea is to split the dataset into training and test sets, which are used to train and validate the model, respectively. CV not only reduces overfitting but also can obtain from the limited dataset more information that is effective. Fig. 10 depicts that this system uses k-fold cross validation (k-fold CV) to reduce variance by averaging the

test results trained on k different groups. The algorithm's steps are presented below: The main steps are as follows:
(1) Randomly divide the original dataset into k parts by non-repetitive sampling, typically in an even manner.
(2) For each iteration, one of the samples is picked for the testing, and the rest of $k - 1$ the datasets are employed for the training. Previous selections should not be repeated.
(3) Reiterate Step 2 for k times so that each subset has a chance to be employed as the testing set. A model will be attained after each training is run, which is then used to test. The model's assessment metrics are computed and saved.

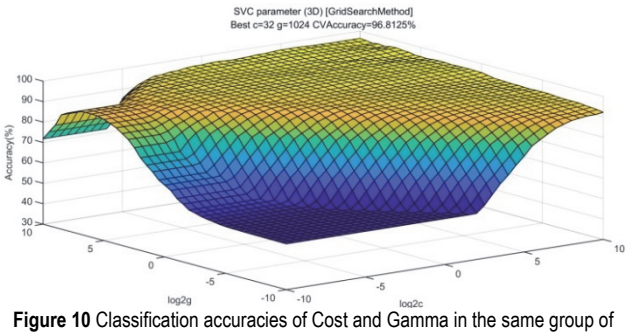

Figure 10 Classification accuracies of Cost and Gamma in the same group of experiments

(4) Compute the mean accuracy of the k tests as the model's predicted accuracy and use it as the performance indicator for the k fold CV of the model.

When the designed system perceiving WSs is on the learning phase perception system, *Label*, the label matrix produced corresponds to F, the feature matrix obtained in section of feature extraction. The element corresponds to a static environment and a dynamic environment set to '0' and to '1', respectively. Therefore, the system's original dataset consists of F and *Label*. The system produces a training model usable for the current room environment by implementing the optimum parameters of C and g for the SVM algorithm. In the testing phase, based on a set of unknown state feature matrices from the same room, the system can train a model to identify the environment state represented by the set of data, thereby achieving indoor personnel detection.

3 EXPERIMENTAL RESULTS

The designed WS perception system aims to identify whether any action occurs inside the room under test and achieve indoor personnel detection in specific application scenarios. For this, this paper conducted the following 2 kinds of experiments and analyzed the outcomes.

(1) The impact of the distance between personnel and testing equipment on the WS's accuracy was explored by the perception system.

(2) The impact of the indoor walls on the accuracy of the system through-wall detection was investigated.

Fig. 11 depicts that the constructed experimental environment realistically simulated an actual scene of a high-rise building fire. The site was an office on the second floor of the building, with an approximate area of 2.7×5.5 m^2. It was measured that the coverage radius of the regular commercial Wi-Fi router was about 12 meters in the office building, so the whole experimentation site was covered by WSs. Most significant behaviors occur within a time frame of a few seconds, so to grasp signals influenced by short-term behaviors, the sampling ratio is set to around 500 samples/s, ensuring a sufficiently high CSI time accuracy to capture details of different human behaviors. If a higher ping frequency was assigned, a higher CSI sampling ratio would be possible. The data packets were collected by the laptop, and CSI was extracted by using the wireless network card.

To assess the personnel detection precision of the wireless human behavior recognition system, we collected the training and test datasets from 4 users for our experiments. The overall dataset collection process was as follows.

(1) Personnel presence detection.

Experiment 1: Impact of distance between user and detection device on system accuracy.

The simulated office on the second floor was ideally selected to have an indoor free space surrounded by some ordinary desks, which is seen as a typical company office in a high-rise building. The equipment layout is shown in Fig. 12, where the heights of the wireless router and laptop were almost equal. The distance parameter d refers to the perpendicular distance between the user and the line connecting the wireless router and the laptop. According to the size of the office space, three regions were divided, with a d of [0, 2 m], (2 m, 4 m], and (4 m, 5.5 m], respectively. The experimentation assessed whether the user in the room moved. Within each distance interval, the user presented two types of states: one was to remain stationary, and the other was to move continuously (without any requirements for the type of action), Collect 20 s of data at each cycle, and acquire 10 sets of data for each type of state.

According to Tab. 1, the designed system achieved an average accuracy of 96.28% in wireless personnel detection within a range of 5.5 m. As the distance between the user and detection devices increased, the recognition accuracy decreased, that is, the system accuracy was inversely proportional to the distance. Nevertheless, the decrease in accuracy was not significant since the room with a size of 5.5 m was at the center of the indoor Wi-Fi coverage (radius of 12 m). In other words, the human behavior's impact on the propagation path of the WS was not pronounced within each distance range.

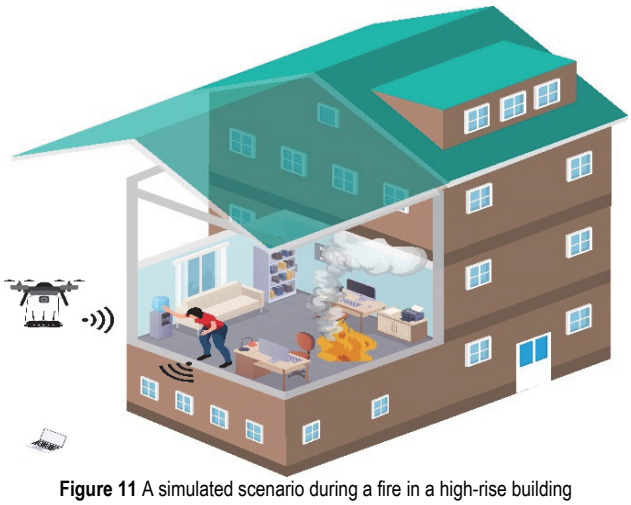

Figure 11 A simulated scenario during a fire in a high-rise building

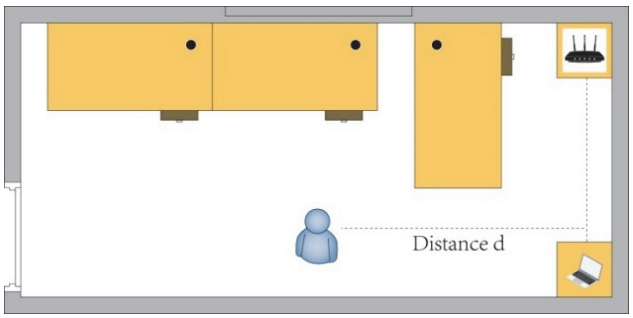

Figure 12 Equipment layout of experiment 1

Table1 Accuracies of system identification under different distances

	Static environment accuracy	Dynamic environment accuracy	Classification accuracy
[0, 2]	99.80%	97.50%	98.60%
(2, 4]	99.00%	97.20%	97.50%
(4, 5.5]	96.00%	89.50%	92.75%
Mean accuracy	98.27%	94.73%	96.28%

Experiment 2: Impact of wall penetration on system detection accuracy.

The equipment layout of experiment 2 is shown in Fig. 13. When the wireless router, which served as the transmitter, was taken off by an unmanned aerial vehicle (UAV) and brought outdoors on the 2-nd floor, the laptop which served as the receiver was placed indoors on the 2-nd floor, made the WS pass through the cement wall in one direction. Besides the concrete, the wall contained another two structures, glass and wooden doors. Generally speaking, WSs experience varying degrees of energy loss after crossing obstacles. Tabl. 2 lists the degree of attenuation for 2.4 GHz WSs after a unidirectional crossing of the building materials involved in this experiment. To verify the impact of walls on the accuracy of system detection, this paper also set up an experiment for comparison: the wireless router position remained unchanged, while the laptop was placed at outdoor location 1 and indoor location 2 respectively. The distances between laptop location 1 and location 2 to the wireless router were kept the same *h*. Under both deployment schemes, the user either remained stationary or continuously made movements (the action types were not specified). In the experiment without penetrating the wall, data was collected for 20 s each time, and 10 sets of data were collected for each kind of state. However, to collect the same number of data files in the through-wall case, the collection time needed to be extended to 50 seconds each time. This was due to the wall reflections of the WS, so the CSI collection tool could not achieve data collection at a high sampling rate. It is worth noting that this system did not distinguish between static situations where the indoor personnel did not move and those where no one was present.

According to Tab. 3, the average detection accuracy of the designed system reached 94.60% after wall penetration. Under this wall penetrating scenario, the recognition accuracy decreased for dynamic environments but increased for static environments. This was because wall reflections decreased the actual sampling rate, resulting in reduced frequency components in the collected data and insufficient CSI sensitivity to the environment state. Therefore, the through-wall recognition accuracy was reduced for the environment where actions were present. On the contrary, the through-wall accuracy of the static environment was higher than that without passing through the wall, which was more sensitive to environmental information. It could be inferred that if more layers of walls between the transmitter and receiver were present, the system recognition accuracy of a dynamic environment would also decrease.

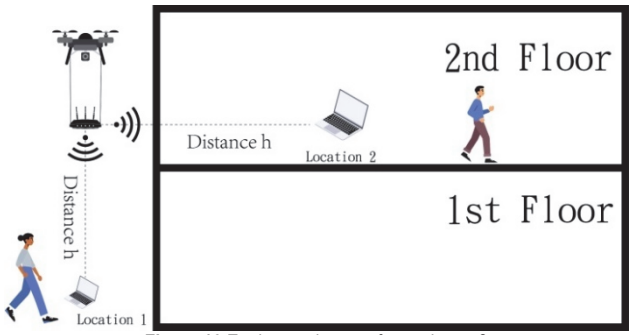

Figure 13 Equipment layout of experiment 2

Table 2 Attenuation of 2.4 GHz WSs after unidirectional passing of different building materials [18]

Building Material	Thickness / inch	2.4 GHz Wireless Signal Attenuation / dB
Glass	/	3
Wooden door	1.75	6
Concrete Wall	18	18

Table 3 Accuracies of system identification in experiment 2 of through-wall detection

	Static environment accuracy	Action detection accuracy	CV classification accuracy
Not penetrating walls	91.80%	97.40%	94.60%
Penetrating walls	98.60%	94.60%	94.60%
Average accuracy	95.20%	96.00%	94.60%

4 CONCLUSION

Unlike other types of fires, high-rise building fires feature a high personnel density, narrow escape routes, rapid-fire spreading, and difficulties in search and rescue. When a fire occurs in an urban high-rise building, its small emergency evacuation exits make it hard for the crowd to escape. Moreover, high-rise buildings mainly use vertical shafts such as elevators as the main passageway, so smoke quickly spreads after a fire. Many people in the building will be trapped in randomly distributed locations, leading to a high search difficulty and a short golden time for rescue. Investigating the impacts of indoor personnel waving for help in fire accidents on wireless channel states, this paper proposed a method to detect indoor personnel using the CSI of WSs. A single-source wireless device combined with signal sampling and SVM was used to perceive and classify wireless channel states, thereby determining if someone was waving for help in a static environment. The experimental outcomes revealed that the proposed approach could perceive the presence of personnel through walls, with an accuracy of 94.6%. The design has the characteristics of non-invasiveness, robustness, universality, and low cost, effectively solving the problems of blind spots, susceptibility to environmental

factors such as smoke, and high equipment costs in video search and rescue systems. It has broad values in improving the efficiency of fire search and rescue.

As research deepens, the following shortcomings of this paper need to be addressed before applying the designed system to more complex practical environments.

(1) More kinds of indoor spaces should be considered to validate the robustness of the proposed wireless indoor personnel perception system with UAV in case of a fire.

(2) The WSs used in this paper had to be Wi-Fi signals following the IEEE 802.11n protocol. Nevertheless, as wireless technology develops, commercially available standard Wi-Fi equipment progressively adopted the more developed 802.11 protocol standards, such as 802.11ac and 802.11ah. So in future research, it is necessary to consider the compatibility of Wi-Fi signal protocols and optimize the system performance with the advanced features of the newer standards.

(3) The receiver used in this system was a laptop computer equipped with an Intel5300 wireless network card, which had a relatively large volume. Future work may explore its miniaturization and adopt a field-programmable gate array (FPGA) embedded mode.

In summary, the designed system for detecting indoor personnel in a fire using wireless perception and UAVs has preliminarily constructed its proof-of-concept model and has been validated in a small controllable space. The system presents a broad spectrum of applications in the future when the wireless perception methods achieve better. It can play a positive role in optimizing search and rescue technology and capabilities in the case of high-rise building fires, which possess important practical values and social significance.

Acknowledgment

This work was supported by Key Program of the National Natural Science Foundation of China (No. 61332019).

5 REFERENCES

[1] Wang, K., Yuan, Y., Chen, M., Lou, Z., Zhu, Z., & Li, R. (2022). A Study of Fire Drone Extinguishing System in High-Rise Buildings. *Fire, 5*(3), 75. https://doi.org/10.3390/fire5030075

[2] Wang, C., Chen, S., Yang, Y., Hu, F., Liu, F., & Wu, J. (2018). Literature review on wireless sensing-Wi-Fi signal-based recognition of human activities. *Tsinghua Science and Technology, 23*(2), 203-222. https://doi.org/10.26599/TST.2018.9010080

[3] Zhao, M. M., Li, T. H., Abu Alsheikh, M., Tian, Y. L., Zhao, H., Torralba, A., & Katabi, D. (2018). Through-wall human pose estimation using radio signals. *Proc. IEEE Conf. Computer Vision and Pattern Recognition*, Salt Lake City, Utah, 7356-7365, IEEE. https://doi.org/10.1109/cvpr.2018.00768

[4] Li, T. H., Fan, L. J., Zhao, M. M., Liu, Y. C., & Katabi, D. (2019). Making the invisible visible: Action recognition through walls and occlusions. *Proc. IEEE/CVF Int. Conf. Computer Vision*, Seoul, Korea, 872-881, IEEE. https://doi.org/10.1109/iccv.2019.00096

[5] Yue, S. C., Yang, Y. Z., Wang, H., Rahul, H., & Katabi, D. (2020). BodyCompass: Monitoring sleep posture with wireless signals. *Proc. ACM Interact. Mob. Wearab. Ubiq. Technol., 4*(2), 1-25. https://doi.org/10.1145/3397311

[6] Fan, L. J., Li, T. H., Fang, R. Y., Hristov, R., Yuan, Y., & Katabi, D. (2020). Learning longterm representations for person re-identification using radio signals. *Proc. IEEE/CVF Conf. Computer Vision Pattern Recognition*, Virtual, 10699-10709, IEEE. https://doi.org/10.1109/cvpr42600.2020.01071

[7] Yu, B. H.,Wang, Y. X., Niu, K., Zeng, Y. W., Gu. T., Wang, L. Y., Guan, C. T., & Zhang, D. Q. (2021). WiFi-sleep: Sleep stage monitoring using commodity Wi-Fi devices. *IEEE Internetof Things Journal, 8*(18), 13900-13913. https://doi.org/10.1109/jiot.2021.3068798

[8] Zhang, L., Wang, C., Ma, M. D., & Zhang, D. Q. (2019). WiDIGR: Direction-independent gait recognition system using commercial Wi-Fi devices. *IEEE Internetof Things Journal, 7*(2), 1178-1191. https://doi.org/10.1109/jiot.2019.2953488

[9] Hang, T. M., Zheng, Y., Qian, K., Wu, C. S., Yang, Z., Zhou, X. C., Liu, Y. H., & Chen, G. L. (2019). WiSH: WiFi-based real-time human detection. *Tsinghua Science and Technology, 24*(5), 615-629. https://doi.org/10.26599/tst.2018.9010091

[10] Wang, B., Liu, X., Wei, B., Jia, R., Gan, X., & Huang, L. (2019). Improved weighted k-nearest neighbor algorithm for wifi fingerprint positioning. *Journal of Xidian University, 46*(5), 41-47.

[11] Zheng, C., Li, G., Chen, H., & Wang, A. (2021). Heart rate monitoring method for 77GHz FMCW radar based on second harmonic weighted reconstruction. *Journal of Xidian University, 48*(2), 173-180.

[12] Yang, S. H., Yuan, Z. M., & Li, W. (2020). Error data analytics on RSS range-based localization. *Big Data Mining and Analytics, 3*(3), 155-170. https://doi.org/10.26599/bdma.2020.9020001

[13] Qian, K., Wu, C. S., Yang, Z., Liu, Y. H., He, F. G., & Xing, T. Z. (2018). Enabling contactless detection of moving humans with dynamic speeds using CSI. *ACM Transactions on Embedded Computing Systems, 17*(2), 1-18. https://doi.org/10.1145/3157677

[14] Song, Z. P., Cao, Z. C., Li, Z. J., Wang, J. L., & Liu, Y. H. (2021). Inertial motion tracking on mobile and wearable devices: Recent advancements and challenges. *Tsinghua Science and Technology, 26*(5), 692-705. https://doi.org/10.26599/tst.2021.9010017

[15] Zhu, J., Rosset, S., Tibshirani, R., & Hastie, T. (2003). 1-norm support vector machines. *Proc. 2003 Neural Information Processing Systems (NIPS) Conf.*, Vancouver, 2003, 16, 49-56, MIT Press.

[16] Zhu, H., Xiao, F., Sun, L. J., Xie, X. H., Yang, P. L., & Wang, R. C. (2017). Robust and passive motion detection with COTS WiFi devices, *Tsinghua Science and Technology, 22*(4), 345-359. https://doi.org/10.23919/tst.2017.7986938

[17] Chang, C. C. & Lin, C. J. (2011). LIBSVM: a library for support vector machines. *ACM Transactions on Intelligent Systems and Technology, 2*(3), 1-27. https://doi.org/10.1145/1961189.1961199

[18] Halperin, D., Hu, W. J., Sheth, A., & Wetherall, D. (2010). 802.11 with multiple antennas for dummies. *ACM Sigcomm Computer Communication Review, 40*(1), 19-25. https://doi.org/10.1145/1672308.1672313

Contact information:

Lin TANG
Key laboratory of Specialty Fiber Optics and Optical Access Networks,
Joint International Research Laboratory of Specialty Fiber Optics and Advanced Communication,
Shanghai University, Shanghai 200444, China

Chao WANG
(Corresponding author)
Key laboratory of Specialty Fiber Optics and Optical Access Networks,
Joint International Research Laboratory of Specialty Fiber Optics and Advanced Communication,
Shanghai University, Shanghai 200444, China
E-mail: wangchao_shu2024@163.com

Yinfan DING
Key laboratory of Specialty Fiber Optics and Optical Access Networks,
Joint International Research Laboratory of Specialty Fiber Optics and Advanced Communication,
Shanghai University, Shanghai 200444, China

Meng ZHOU
Key laboratory of Specialty Fiber Optics and Optical Access Networks,
Joint International Research Laboratory of Specialty Fiber Optics and Advanced Communication,
Shanghai University, Shanghai 200444, China